SAND2016-11047C

Exceptional service in the national interest

Sandia National Laboratories

Characterization of neutron scatter for the 25-m neutron time of flight detector at the Z Accelerator

Edward Norris[1], Kelly Hahn[1], Gordon Chandler[1], Carlos Ruiz[1], Jedediah Styron[2], Gary Cooper[2], Brent Jones[1], Jose Torres[1], Decker Spencer[1], Alan Nelson[1]

[1]Sandia National Laboratories, [2]University of New Mexico

Background and Objective

The neutron time of flight (NTOF) detector along the radial LOS 50 at 25 m at the Z Pulsed Power accelerator has been used on magnetized liner inertial fusion (MagLIF) experiments to measure neutron spectra. After the primary pulse, there is an expected scatter contribution on second half of the signal. However, the experimental and theoretical distributions differ during the first half of the signal which is presently not understood. **We are investigating whether this is due to target physics that affect the spectra or instrumental effects.**

The goals of this project are:

1. Construct a computational MCNP model of the Z facility
2. Identify the most appropriate variance reduction techniques for this problem
3. Identify necessary simplifications to carry out the simulation

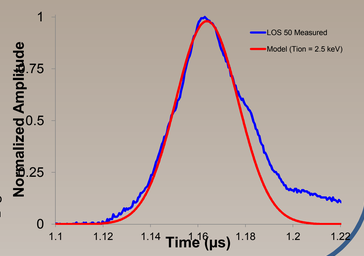

Figure 1. A comparison of the experimentally gathered TOF signal to the theoretically expected signal. Both signals are bang-time corrected.

Methods

The Z Pulsed Power Accelerator was modeled using the MCNP6 code. This code estimates the energy dependent volume averaged energy-time dependent energy deposition inside the TOF detector using a F6 tally. The energy deposition is then converted to the expected light yield using Equation (1).

$$\left[\int F_6(E,t) \times \Gamma(E)dE\right] \otimes R(t) \propto \text{Signal} \quad (1)$$

$$\Gamma(E) = \sum_{i=1}^{N} \Gamma_i(E)\frac{\Sigma_i(E)}{\Sigma_t(E)} \quad (2)$$

MCNP6 directly outputs $F_6(E,t)$ which is then multiplied by a light yield curve, $\Gamma(E)$, shown in Fig. 2, and integrated over all energies. The total light yield is calculated using Equation (2) where each Γ_i is taken from existing empirical correlations for the constituent materials in the detector; Σ_i and Σ_t are the cross sections of the i^{th} material and the total cross section respectively. The result is then convolved with an experimentally measured temporal response, $R(t)$, shown in Fig. 3. Convolving the theoretical light yield with the detector response broadens the signal and performs a smoothing operation producing a more realistic signal.

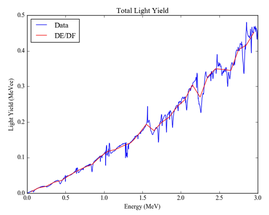

Figure 2. Total light output curve as calculated using Equation (2). The Data trend shows the calculated light yield, the DE/DF trend shows the discretized version used by the MCNP simulation

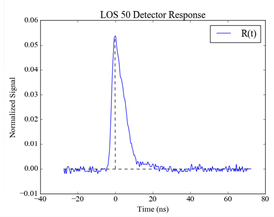

Figure 3. Time response curve for the LOS 50 TOF detector

Model

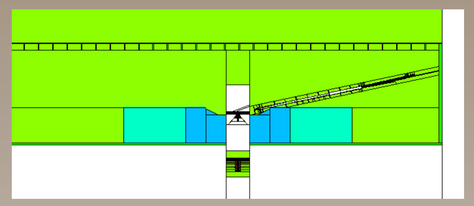

Figure 4. Overview of the Z Pulsed Power Accelerator high bay.

Multiple existing computational MCNP models were combined to create the large model shown in Fig. 4. The center section (Fig. 5) and basement NTOF (Fig. 6) models were constructed previously. One of the key accomplishments of this project was to reconcile the existing models into a single model that captures a much wider picture of the geometry.

The principal high bay geometry was added in, including the oil and water tanks as well as the concrete structural building. Many more details that contribute to the signal are not included, some of which are shown in Fig. 7.

The LOS 50 model itself was created by pulling dimensions off of an existing SolidWorks model. A comparison of the two is shown in Fig. 8.

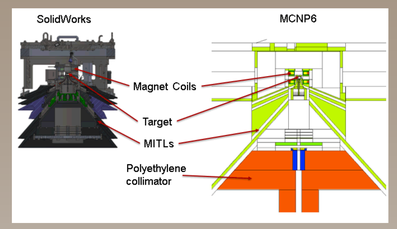

Figure 5. A close-up view of the center section in Fig. 4, modeled by Kelly Hahn.

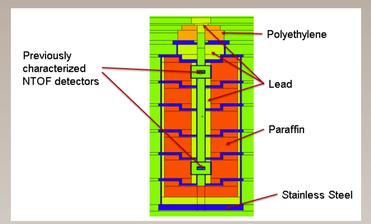

Figure 6. The basement TOF pig previously modeled by Alan Nelson

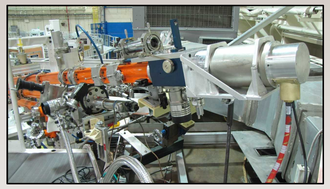

Figure 7. Photograph of the current LOS 50 NTOF detector at the time of writing. Note that there are numerous hardware components currently on the LOS for retired diagnostic systems. These components attenuate the neutron signal and contribute to scatter in the observed signal.

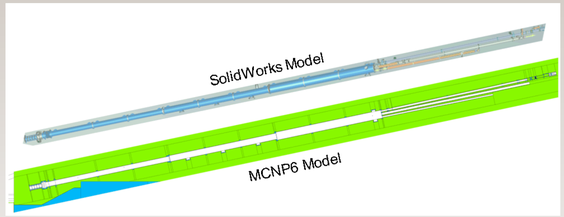

Figure 8. A comparison of the LOS 50 MCNP model to the SolidWorks model from which dimensions were pulled.

Computational Acceleration

Due to the distance between the target chamber and the NTOF detector, as well as scattering caused by hardware along the LOS from other diagnostics, the fraction of source particles reaching the detector is very small, O(10^{-7}). In order to achieve statistically meaningful results, an untenably large number of particles needs to be run, necessitating the supercomputing resources available for simulation at Sandia.

To overcome the large runtimes needed, a weight window map was used. The weight window map was generated by MCNP6 using the built-in weight window generator. Fig. 9 shows a plot of the weight window values overlaid with the geometry. The geometry was rotated 12.7 degrees so that LOS50 aligned with the x-axis; this allowed a courser weight window mesh to accurately capture the significant geometry.

In addition to the weight window map, a cone bias source was used to preferentially bias particles down the LOS toward the detector. The motivation for using both a cone bias and a weight window map was the idea that the cone bias would propagate particles down the LOS and the weight windows would capture scatter everywhere else. Typical results such as those shown in Fig. 10 required approximately 24000 computer hours distributed across 128 nodes on Sandia's Skybride cluster.

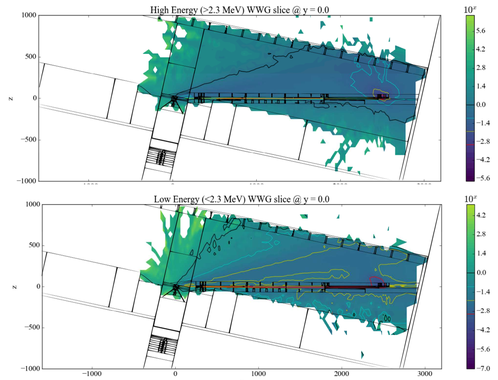

Figure 9. Weight window maps produced by the built-in MCNP6 weight window generator. These maps were used to decrease the runtime required by the simulation.

Results and Conclusions

The MCNP6 simulated LOS 50 NTOF signal is plotted in Fig. 10 and the corresponding uncertainty is shown in Fig. 11. Figure 10 also shows an experimental curve against which the MCNP6 results are compared.

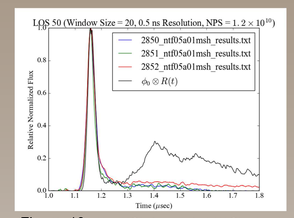

Figure 10. The MCNP predicted NTOF signal compared two three experimental MagLIF shot datasets, namely Z2850, Z2851, and Z2852.

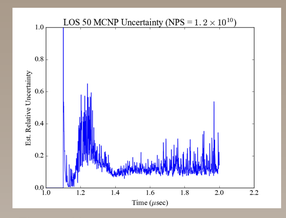

Figure 11. The statistical uncertainty in the MCNP estimated signal given in Fig. 10.

Enlarging the region of interest in Fig. 10 reveals, in Fig. 11, that the MCNP agrees well on the rising edge of the pulse, but is reduced too rapidly on the falling edge. These results indicate that including the burn time in the simulation may improve the agreement significantly. The results in Fig 10 have had a 20 bin moving average applied to reduce noise.

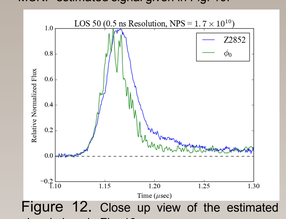

Figure 12. Close up view of the estimated signal given in Fig. 10.

Discussion and Future Work

The simulation results agree somewhat in the primary peak region but disagree in the downscattered region. Analyzing the importance maps in Fig. 9 reveal that there is a significant contribution of downscatter off of the concrete ceiling and walls. Further investigation reveals that about 90% of the scatter is from the concrete; a comparison of the total neutron flux to the contribution from any scatter in concrete is shown in Fig. 13. The exaggerated fraction of scatter off of the concrete structures indicates that some attenuating features of the Z high bay are not currently included in the model. The most likely culprits at the moment are other sources of scatter from hardware not yet incorporated into the model.

There are a number of future improvements that will be made to this model including:

1. addition of other hardware near the detector (screenroom)
2. addition of further geometry at the top of the center section
3. including the beryllium liner present in MagLIF shots
4. Improved variance reduction so more particles can be reliably run

Once these improvements are made, the model will be leveraged to design improved collimation for LOS 50. Such a modification will help determine critical target physics parameters such as ion temperature.

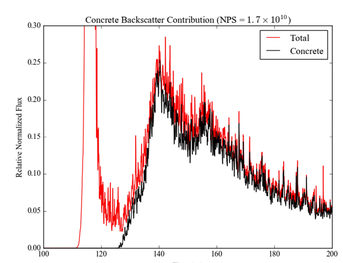

Figure 13. Comparison of the total (normalized) flux to the flux having passed through a concrete structure (floor, ceiling, and walls). The concrete contribution was calculated in MCNP by the use cell flagging